Journal of Computational Physics 227 (2008) 10058–10077

Contents lists available at ScienceDirect

Journal of Computational Physics

journal homepage: www.elsevier.com/locate/jcp

Generalized Roe schemes for 1D two-phase, free-surface flows over a mobile bed

G. Rosatti [a,*], J. Murillo [b,1], L. Fraccarollo [a]

[a] Centro Universitario per la Difesa idrogeologica dell'Ambiente Montano (CUDAM), Dipartimento Ingegneria Civile e Ambientale, Università degli Studi di Trento, Via Mesiano, 77 I-38050 Trento, Italy
[b] Área de Mecánica de Fluidos, Centro politecnico Superior, Universitad de Zaragoza, Maria de Luna 3, 50015 Zaragoza, Spain

ARTICLE INFO

Article history:
Received 19 May 2008
Received in revised form 8 August 2008
Accepted 11 August 2008
Available online 22 August 2008

Keywords:
Two-phase flows
Free-surface
Mobile bed
Nonconservative product
Generalized Roe solvers
Weak solutions
Well-balanced approach

ABSTRACT

The problem of two-phase, free-surface flows over a mobile bed is characterized by a hyperbolic partial differential equations system that shows nonconservative terms and highly nonlinear relations between primitive and conserved variables. Weak solutions of the present problem were obtained resorting both to the distribution theory and to the integral formulation of momentum conservation: the comparison of these two approaches allowed us to give a physical insight into the meaning of the nonconservative term across a discontinuity. Starting from this result, we derived the conditions necessary to obtain generalized, well-balanced Roe solvers without using the concept of a family of paths. Two numerical schemes based on the same set of matrices have been developed, one in terms of conserved variables and one in terms of primitive variables. The friction-source term has also been included by using an upwind approach. The capabilities and limits of the proposed schemes have been analyzed by comparison with exact solutions of Riemann problems and with numerical solutions obtained with the AWB-3SRS scheme.

1. Introduction

Water flows in mountain regions are frequently connected with heavy sediment movements that generate significant erosional and depositional processes. Debris flows and dam-breaks over mobile beds are the most widely studied phenomena of this type. The quantity of sediment that can be transported in these flows is such that it is more appropriate to describe these phenomena as flows of a mixture of water and sediments instead of considering water flows with a negligible contribution of the transported sediments in terms of mass and momentum. Moreover, the exchange of sediments from the bed to the flow and vice-versa is such that the bed variations have the same time-scale as the free-surface variations. The mathematical description of flows with high sediment transport is therefore rather different from the equation system used in the case of sediment transport in rivers and shows peculiarities which are rather challenging from a numerical point of view. Despite a significant increase in both interest and research in recent years, knowledge of the phenomenon is not complete and therefore several different mathematical models can be found in existing literature, each with its own features [14,15,3,5]. In this paper we focus our attention only on a specific model already used by some of the authors [22,2], leaving the problem of development, validation and discussion of mathematical models for these types of flows to other scientific communities.

The aim of this paper is exclusively numeric: it consists in the development of generalized Roe approaches for the assumed mathematical model and in the analysis of the performances of these new numerical schemes. Roe schemes have

* Corresponding author. Tel.: +39 0461882621; fax: +39 0461882672.
E-mail addresses: giorgio.rosatti@ing.unitn.it (G. Rosatti), Javier.Murillo@unizar.es (J. Murillo), luigi.fraccarollo@ing.unitn.it (L. Fraccarollo).
[1] The present work was developed during a research period at CUDAM, Italy.

0021-9991/$ - see front matter © 2008 Elsevier Inc. All rights reserved.
doi:10.1016/j.jcp.2008.08.007

already been employed in some works regarding debris flows and ordinary mobile-bed flows. Specifically, [3] applied this approach to a model that can be considered a rather simplified version of that assumed in this paper; [13] used Roe schemes for solving one-dimensional shallow-water equations with sediment transport and bed evolution; [9] extended the approach of [13] by using ENO-WENO methodology and linearizing the nonconservative term present in the system of equations. Nevertheless the numerical problems examined in this paper are rather different from those present in the above-mentioned papers: the hyperbolic PDEs system is much more complex, it presents a nonconservative term that cannot be simply linearized or treated as a source term, and furthermore the relation between primitive and conserved variables is highly nonlinear.

As we will show in the following section, the development of generalized Roe approaches for the present problem cannot follow the results available in the literature based on the distribution theory approach [27,19,20,7]. Instead, generalized Rankine–Hugoniot relations have been obtained in [22] writing the integral formulation of the momentum conservation principle for a moving frame with velocity equal to the shock speed S_s (physical approach). This result has been used in order to develop generalized Roe solvers. The basic path we have taken is as follows: we went back to the original ideas of Roe, rewrote the original conditions in terms of generalized expressions and finally found a suitable matrix (or matrices) fulfilling the constraints. Unfortunately, the approaches we obtained, one in terms of primitive variables and one in terms of conserved variables, are not completely general and cannot be applied straightforwardly to all nonconservative hyperbolic systems. Nevertheless, they may become useful frameworks for developing generalized Roe solvers in cases in which generalized Rankine–Hugoniot relations are available from integral conservation principles. Finally, the numerical schemes we present are only first-order accurate because in this way the peculiarities of the methods are made clear. Extension to higher orders will be a goal of our future work.

The outline of the paper is as follows: in Section 2, we present the integral and differential formulations of the mathematical model, the features of the relevant weak solutions and of the relevant Riemann Problems (hereafter RPs). In Section 3, the conditions necessary for obtaining well-balanced, generalized Roe solvers as well as the relevant matrices are developed first for a conserved-variable approach, then for a primitive-variable approach. The section ends with the treatment of the source friction term and the stability condition for the methods. In Section 4, the capabilities and limits of the proposed schemes are analyzed by comparison of the numerical results with exact solutions of RPs and with the numerical results of the AWB-3SRS scheme [22]. The paper closes with some conclusions.

2. The mathematical model and its features

In this section, we briefly present the mathematical model adopted in this work with its peculiarities. The phenomena we are interested in regard highly erosive free-surface flows propagating over loose beds of coarse, cohesionless sediments. They can be encountered in various conditions of geomorphological and engineering interest ranging from valley-forming floods, to debris flows in mountainous terrain. Other remarkable cases regard laboratory studies of dam-break flows over a mobile bed.

The model involves the following assumptions: (i) shallow-water approach: the flow is oriented in a predominantly horizontal direction and is confined to a layer which is thin compared to the horizontal scale of interest; (ii) two-phase flow: the mixture of water and sediments is described by using the continuum approach and assuming the same velocity for the liquid and for the solid phase; (iii) morphodynamic interface: the bed boundary Γ_b is viewed as a phase interface across which the liquid-granular mixture undergoes a transition from fluid- to solid-like behaviour; above Γ_b the mixture is assumed to flow as a fluid, while a solid-like behaviour is considered below this level (i.e. a rigid granular skeleton through which groundwater seepage is neglected). Erosion occurs as the bed boundary progresses downwards while deposition results when the boundary moves up. For more details on the physical and theoretical framework used to work out the model we refer to [11] and to [22] for the demonstration of the mathematical properties of the model.

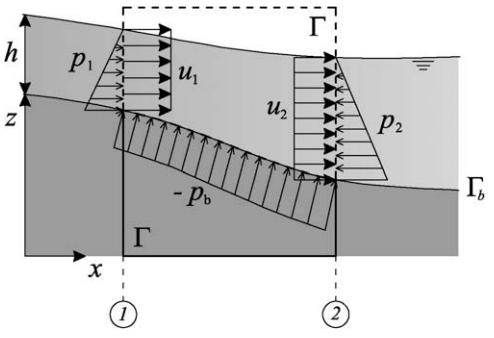

Fig. 1. Control volume for the determination of the integral equations of flow over mobile-bed with high sediment transport.

Considering a generic control volume Γ (Fig. 1), the relevant integral formulation of the model derives, respectively, from the depth-averaged equation of bulk mass conservation, conservation of the solid phase mass and conservation of the mixture momentum. In a Cartesian coordinate system (x,z) with a horizontal x-axis and a vertical z-axis, this becomes:

$$\frac{\partial}{\partial t}\int_{x_1}^{x_2}\mathbf{U}\,\mathrm{d}x+\mathbf{F}|_{x_2}-\mathbf{F}|_{x1}-\int_{x_1}^{x_2}\mathbf{P}\,\mathrm{d}\Gamma_\mathrm{b}=\int_{x_1}^{x_2}\mathbf{R}\,\mathrm{d}\Gamma_\mathrm{b} \tag{1}$$

where x_1, x_2 are the limits of the control volume Γ, Γ_b is the line defining the bed, and the vectors are, respectively

$$\mathbf{U}=\begin{pmatrix} h+z \\ ch+c_\mathrm{b}z \\ (c\Delta_\rho+1)uh \end{pmatrix},\quad \mathbf{F}=\begin{pmatrix} hu \\ chu \\ (c\Delta_\rho+1)(u^2h+\frac{1}{2}gh^2) \end{pmatrix}, \tag{2}$$

$$\mathbf{P}=\begin{pmatrix} 0 \\ 0 \\ \frac{p_\mathrm{bx}}{\rho_\mathrm{w}} \end{pmatrix},\quad \mathbf{R}=\begin{pmatrix} 0 \\ 0 \\ -\frac{\tau_x}{\rho_\mathrm{w}} \end{pmatrix}, \tag{3}$$

where h is the mixture depth, u is the depth averaged velocity, c is the volume concentration of sediments, c_b is the concentration of sediments in the bed ($c<c_\mathrm{b}$), z is the bed elevation, g is gravity, $\Delta_\rho=(\rho_\mathrm{s}-\rho_\mathrm{w})/\rho_\mathrm{w}$ is the relative buoyant density of the sediments, ρ_s is the density of the solid phase and ρ_w is the density of the water. Finally, p_bx, τ_x are, respectively, the x-component of the pressure and of the shear stress exerted on the bed.

As far as the closure relation is concerned, we assumed the immediate adaptation hypothesis which considers an algebraic relation between the local and instantaneous values of the physical variables and the concentration. The expression used in this work is:

$$c=c_\mathrm{b}\gamma\frac{u^2}{h}, \tag{4}$$

where γ is an empirical parameter [25]. As for the bed shear stress τ, it can be replaced by using any expression for open-channel hydraulics or for debris-flow rheology [26,3,2].

From a physical point of view, the peculiarity of this model, as compared to sediment-transport models, lies in the momentum equation: when the sediment concentration is low (as commonly happens in standard sediment transport conditions) concentration is negligible and the equation degenerates to the standard shallow-water momentum equation. Moreover, since in this case the bed variations are small and rather smooth, decoupling of the hydrodynamic system from the bed elevation equation is commonly assumed and the pressure on the bed is expressed by a smooth function. When on the other hand concentration is high (as in debris-flow situations), there is a strong interaction between the two phases and between the mixture and the bed, and so no decoupling can be considered. Moreover, since the bed variations may be large, appropriate treatment of the pressure term over discontinuities is mandatory.

The differential formulation of the mathematical model can be obtained assuming smooth variation of the variables and an infinitesimal width of the control volume. In these conditions, the pressure term becomes:

$$\frac{p_\mathrm{bx}}{\rho_\mathrm{w}}=-gh(c\Delta_\rho+1)\frac{\partial z}{\partial x}, \tag{5}$$

while the PDEs system is reduced to:

$$\frac{\partial\mathbf{U}}{\partial t}+\frac{\partial}{\partial x}\mathbf{F}(\mathbf{U})+\mathbf{H}\frac{\partial z}{\partial x}=\mathbf{R}, \tag{6}$$

where

$$\mathbf{H}=\begin{bmatrix}0 & 0 & gh(c\Delta_\rho+1)\end{bmatrix}^\mathrm{T} \tag{7}$$

It can be demonstrated [26] that the system (6) is strictly hyperbolic: two eigenvalues have the same sign as the particle velocity u while one is opposite. We name them in ascending order: with $u>0$, $\lambda^1<0$, $\lambda^2\geqslant 0$, $\lambda^3>0$ and $\lambda^3>\lambda^2$, while $\lambda^2=0$ only if $u=0$, i.e. the condition of fluid at rest. λ^1 and λ^3-characteristic fields are genuinely nonlinear while the λ^2-characteristic field is linearly degenerate only for the condition of water at rest, while it remains nonlinear for any other value of the variables.

2.1. Weak solutions

Because of the presence of a nonconservative term, the definition of a weak solution for the hyperbolic system (6) is not straightforward.

2.1.1. The theoretical–mathematical approach

The first way to obtain a definition of a weak solution for a general nonconservative hyperbolic system is by resorting to the distribution theory. For a detailed treatment of the topic we refer to [8,16,10]. Here we will give only a brief overview of

this approach yielding a generalized expression of the Rankine–Hugoniot relation. We will then apply this approach to our specific problem.

Following [10], given a generic nonconservative product $\mathbf{f}(\mathbf{U})(\partial\mathbf{U}/\partial x)$, where $\mathbf{f}:\mathbb{R}^m\to\mathbb{R}^m$ is a smooth function and $\mathbf{U}$ is a function of bounded variation, its value across a discontinuity, with left and right values $\mathbf{U}_L,\mathbf{U}_R$, respectively, can be defined by means of a Borel measure:

$$\mu=\int_0^1 \mathbf{f}(\mathbf{\Phi}(s;\mathbf{U}_L,\mathbf{U}_R))\frac{\partial\mathbf{\Phi}}{\partial s}(s;\mathbf{U}_L,\mathbf{U}_R)\mathrm{d}s=\mathbf{f}(\mathbf{U})\frac{\partial\mathbf{U}}{\partial x}, \tag{8}$$

where $\mathbf{\Phi}(s;\mathbf{U}_L,\mathbf{U}_R)$, called a family of paths, is a Lipschitz map $\mathbf{\Phi}:[0,1]\times\mathbb{R}^m\times\mathbb{R}^m\to\mathbb{R}^m$ satisfying certain properties of consistency and regularity. In particular:

$$\mathbf{\Phi}(0;\mathbf{U}_L,\mathbf{U}_R)=\mathbf{U}_L,\quad \mathbf{\Phi}(1;\mathbf{U}_L,\mathbf{U}_R)=\mathbf{U}_R. \tag{9}$$

The value of the measure (8) depends on the particular choice of the family of paths. Given a generic nonconservative hyperbolic problem

$$\frac{\partial\mathbf{U}}{\partial t}+\mathbf{f}(\mathbf{U})\frac{\partial\mathbf{U}}{\partial x}=0, \tag{10}$$

a discontinuous solution $\mathbf{U}(x,t)$ is a weak solution of (10) if and only if, across the discontinuity moving at a speed S_s, it satisfies the following generalized Rankine–Hugoniot condition:

$$\int_0^1 (S_s\mathbf{I}-\mathbf{f}(\Phi(s;\mathbf{U}_L,\mathbf{U}_R)))\frac{\partial\mathbf{\Phi}}{\partial s}(s;\mathbf{U}_L,\mathbf{U}_R)\mathrm{d}s=0, \tag{11}$$

where $\mathbf{I}$ is the identity matrix. It must be noticed that given $\mathbf{U}_L,\mathbf{U}_R$, the speed of the shock depends, in general, on the particular choice of the family of paths. If on the other hand $\mathbf{f}(\mathbf{U})$ is the Jacobian matrix of a flux function $\mathbf{F}(\mathbf{U})$, the previous relation reduces to the standard Rankine–Hugoniot relation regardless of the choice of the family of paths.

Now, turning to our problem, it is not easy to rewrite the homogeneous part of the system (6) in a nonconservative form as (10) because the pressure term depends on the spatial derivative of a primitive variable and not on the spatial derivatives of the conserved variables. Nevertheless, formally, the following expression can be written:

$$\frac{\partial\mathbf{U}}{\partial t}+(\mathbf{J}(\mathbf{U})+\mathbf{H}'(\mathbf{U}))\frac{\partial\mathbf{U}}{\partial x}=\mathbf{0}, \tag{12}$$

where $\mathbf{J}(\mathbf{U})=\partial\mathbf{F}/\partial\mathbf{U}$ and $\mathbf{H}'(\mathbf{U})$ is a suitable matrix. The generalized Rankine–Hugoniot relation becomes:

$$\int_0^1 (S_s\mathbf{I}-\mathbf{J}(\Phi(s;\mathbf{U}_L,\mathbf{U}_R))-\mathbf{H}'(\Phi(s;\mathbf{U}_L,\mathbf{U}_R)))\frac{\partial\mathbf{\Phi}}{\partial s}(s;\mathbf{U}_L,\mathbf{U}_R)\mathrm{d}s=0.$$

Using the property (9) and considering that $\mathbf{J}(\mathbf{U})$ is a Jacobian matrix, the previous relation reduces to:

$$\mathbf{F}_R-\mathbf{F}_L-\mathbf{D}=S_s(\mathbf{U}_R-\mathbf{U}_L), \tag{13}$$

where

$$\mathbf{D}=\int_0^1 \mathbf{H}'(\Phi(s;\mathbf{U}_L,\mathbf{U}_R))\frac{\partial\mathbf{\Phi}}{\partial s}(s;\mathbf{U}_L,\mathbf{U}_R)\mathrm{d}s. \tag{14}$$

This last expression can also be written in terms of the following vector of primitive variables:

$$\mathbf{W}=(h,q,z)^{\mathrm{T}}, \tag{15}$$

where $q=uh$. Relation (14) becomes:

$$\mathbf{D}=\int_0^1 \mathbf{H}(\psi(s;\mathbf{W}_L,\mathbf{W}_R))\frac{\partial\psi}{\partial s}(s;\mathbf{W}_L,\mathbf{W}_R)\mathrm{d}s, \tag{16}$$

where $\psi(s;\mathbf{W}_L,\mathbf{W}_R)$ is another family of paths from $\Phi(s;\mathbf{U}_L,\mathbf{U}_R)$. Unfortunately, the physical meaning of this quantity is not given by the theoretical mathematical approach.

2.1.2. The physical approach

There is another way in this problem to obtain the shock relation that the weak solution must satisfy. It can be obtained by writing the integral formulation of the problem (1) for a moving frame with velocity equal to the shock speed S_s (see Fig. 2). What can be obtained (see [22] for the demonstration) is a relation formally equal to (13), where

$$\mathbf{D}=\left(0,0,\int_{z_L}^{z_R}\frac{p_{bx}}{\rho_w}\mathrm{d}z\right)^{\mathrm{T}}. \tag{17}$$

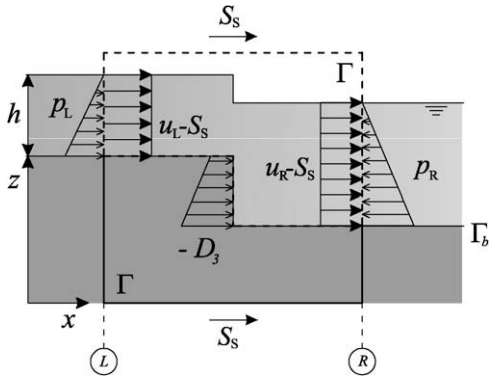

Fig. 2. Mobile control volume for the determination of the shock relations in flows over mobile-bed with high sediment transport. The velocity of the the control volume is equal to the shock speed S_s..

The physical meaning of **D** is now completely clarified: the only nonnull term represents the integral of the mixture pressure on the bottom step divided by the water density, i.e. it is a thrust term. Its evaluation would actually require knowledge of the two-dimensional flow around the bottom step. Reasonable assumptions may nonetheless be made in a one-dimensional framework. In the following, we assume, as in [22], that the pressure distribution in the mixture is hydrostatic over the step and that the pressure head depends only on the free-surface level on either side of the discontinuity where the bottom elevation is lower. Then, the expression of the thrust becomes:

$$D_3 = -g(c_k\Delta_\rho + 1)\left(h_k - \frac{|z_R - z_L|}{2}\right)(z_R - z_L) \quad \text{with } k = \begin{cases} L & \text{if } z_L \leqslant z_R \\ R & \text{otherwise} \end{cases}. \tag{18}$$

The soundness of this assumption should be validated against laboratory experiments, although this is a matter which lies beyond the scope of this paper.

Comparing (14) and (16) with (17) and (18) it becomes clear that we know now the value of the integral but we don't know the expression of the specific paths $\Phi(s;\mathbf{U}_L,\mathbf{U}_R)$ or $\psi(s;\mathbf{W}_L,\mathbf{W}_R)$. It would be desirable to work out their analytical expression but unfortunately, this result is still not available. Consequently, all the theory available from the literature for developing generalized, well-balanced Roe approaches (see e.g. [27,19,20,7]) cannot be applied to the present case in a straightforward manner.

2.2. Integral property of the RP solution

In the following, we derive an integral property of the RP solution that will be used further on to obtain approximate Riemann solvers for the homogeneous part of (6). Given a Riemann problem with initial values $\mathbf{U}_L, \mathbf{U}_R$, a time interval $[0,1]$ and a space interval $[-X,X]$, where

$$-X \leqslant S_L, \quad X \geqslant S_R \tag{19}$$

and S_L, S_R are the positions of the slowest and the fastest wave at $t = 1$, the solution $\mathbf{U}$ at time $t = 1$ satisfies the following property:

$$\int_{-X}^{+X} \mathbf{U}(x,1)\mathrm{d}x = X(\mathbf{U}_R + \mathbf{U}_L) - (\mathbf{F}(\mathbf{U}_R) - \mathbf{F}(\mathbf{U}_L)) + \int_0^1 \int_{-X}^{+X} \mathbf{P}\,\mathrm{d}\Gamma_b\,\mathrm{d}t. \tag{20}$$

This can easily be obtained integrating in time Eq. (1) and using a control volume $[-X,X]\times[0,1]$. The spatial integral of **P** can formally be evaluated using Eq. (5) where the solution is smooth, and Eq. (17) where the solution is discontinuous. It must be noticed that the last integral in the previous equation is not time-independent because of the specific assumption (18).

It is worth comparing the previous expression with that which can be obtained using the distribution theory. Integration over $[-X,X]\times[0,1]$ Eq. (6) in the sense of distributions gives:

$$\int_{-X}^{+X} \mathbf{U}(x,1)\mathrm{d}x = X(\mathbf{U}_R + \mathbf{U}_L) - (\mathbf{F}(\mathbf{U}_R) - \mathbf{F}(\mathbf{U}_L)) + \int_0^1 \left(\sum_{j=0}^{3} \int_0^1 \mathbf{H}'(\Phi(s;\mathbf{U}_j,\mathbf{U}_{j+1}))\frac{\partial \mathbf{\Phi}}{\partial s}(s;\mathbf{U}_j,\mathbf{U}_{j+1})\mathrm{d}s\right)\mathrm{d}t, \tag{21}$$

where $\mathbf{U}_j$ represents the value of the conserved variables in the jth field of the RP solution, $\mathbf{U}_0 = \mathbf{U}_L, \mathbf{U}_3 = \mathbf{U}_R$ and $\Phi(s;\mathbf{U}_j,\mathbf{U}_{j+1})$ represents a family of paths connecting two subsequent intermediate states. If we assume that the union of $\Phi(s;\mathbf{U}_j,\mathbf{U}_{j+1}), j = 0,3$ gives the path $\Phi(s;\mathbf{U}_L,\mathbf{U}_R)$, the equation becomes:

$$\int_{-X}^{+X} \mathbf{U}(x,1)\mathrm{d}x = X(\mathbf{U}_R + \mathbf{U}_L) - (\mathbf{F}(\mathbf{U}_R) - \mathbf{F}(\mathbf{U}_L)) + \int_0^1 \mathbf{H}'(\Phi(s;\mathbf{U}_L,\mathbf{U}_R))\frac{\partial \mathbf{\Phi}}{\partial s}(s;\mathbf{U}_L,\mathbf{U}_R)\mathrm{d}s, \tag{22}$$

where the last integral in (21) is time-independent. This expression is commonly assumed in many papers (see e.g. [27,19,20,7]) however, comparing this equation with Eq. (20) we can conclude that in our specific problem, the approaches available in the literature do not apply in a straightforward manner.

3. Generalized Roe approaches

We recall here the basic steps we used to develop generalized Roe solvers for the present problem: we went back to the original ideas of Roe, rewrote the original conditions in terms of generalized expressions and finally found a suitable matrix (or matrices) fulfilling the constraints. In the present section, we will apply this methodology starting from the formulation of the problem both in terms of conserved variables and in terms of primitive variables.

3.1. The consistency condition

In order to obtain a numerical solution of system (6) we divide the domain in computational cells of a constant size Δx: the interval of the ith cell is defined by $[x_{i-1/2}, x_{i+1/2}]$ where $x_{i+1/2} = i\Delta x$ and the position of the center of the cell x_i is defined by $(i-1/2)\Delta x$. Let Δt be the time step and $t^n = n\Delta t$ a generic time; assuming the usual notation we indicate with $\mathbf{U}_i^n$ the cell-average value of the solution $\mathbf{U}(x,t)$ for the ith cell at time t^n:

$$\mathbf{U}_i^n = \frac{1}{\Delta x}\int_{x_{i-1/2}}^{x_{i+1/2}} \mathbf{U}(x,t^n)\mathrm{d}x. \tag{23}$$

$\mathbf{U}_i^n$ is therefore a piecewise approximation of the solution at time t^n. We first consider the update algorithm for the homogeneous part of the system (6) delaying the treatment of the source term up to Section 3.4.

The Godunov method, in its first-order formulation, provides a way to update the averaged quantities at a new time step in the following way: the variable steps that are obtained at the side of the cells with the piecewise approximation (23), are considered as initial values of local RPs:

$$\left.\begin{array}{l} \frac{\partial \mathbf{U}}{\partial t} + \frac{\partial \mathbf{F}}{\partial x}(\mathbf{U}_i^n, \mathbf{U}_{i+1}^n) = 0 \\ \mathbf{U}(x,0) = \begin{cases} \mathbf{U}_i^n & \text{if } x < 0 \\ \mathbf{U}_{i+1}^n & \text{if } x > 0 \end{cases} \end{array}\right\}. \tag{24}$$

These RPs are then evolved for a time equal to the time step; the resulting solution is cell-averaged again obtaining the piecewise solution at the new time level t^{n+1}.

In the Roe approach, the solution of each RP is obtained from the exact solution of a locally linearized problem. This solution must fulfill the so-called consistency condition, i.e. that the integral of the solution $\widehat{\mathbf{U}}(x,t)$ of the linearized RP over a suitable control volume must be equal to the integral of the exact solution of (24) over the same control volume. Using (20) this condition becomes:

$$\int_{-X}^{+X} \widehat{\mathbf{U}}(x,1)\mathrm{d}x = X(\mathbf{U}_\mathrm{R} + \mathbf{U}_\mathrm{L}) - (\mathbf{F}(\mathbf{U}_\mathrm{R}) - \mathbf{F}(\mathbf{U}_\mathrm{L})) + \int_0^1 \int_{-X}^{+X} \mathbf{P}\,\mathrm{d}\Gamma_\mathrm{b}\,\mathrm{d}t. \tag{25}$$

Since the pressure is not constant in time, we assume the following time linearization of the consistency condition:

$$\int_{-X}^{+X} \widehat{\mathbf{U}}(x,1)\mathrm{d}x = X(\mathbf{U}_{i+1} + \mathbf{U}_i) - (\mathbf{F}(\mathbf{U}_{i+1}) - \mathbf{F}(\mathbf{U}_i) - \mathbf{D}_{i+1/2}), \tag{26}$$

where

$$\mathbf{D}_{i+1/2} = \int_{-X}^{+X} \mathbf{P}(x,0)\mathrm{d}\Gamma_\mathrm{b}$$

is the thrust term associated with the initial condition $\mathbf{U}(x,0)$ of the side RP. It must be noticed that this assumption is exact in case of fluid at rest but the impact of this approximation will be evident in the section concerning the numerical tests.

3.2. The generalized Roe scheme in terms of conserved variables

In this formulation, RP (24) is approximated by using the following linear RP:

$$\left.\begin{array}{l} \frac{\partial \widehat{\mathbf{U}}}{\partial t} + \widetilde{\mathbf{J}}(\mathbf{U}_i, \mathbf{U}_{i+1})\frac{\partial \widehat{\mathbf{U}}}{\partial x} = 0 \\ \widehat{\mathbf{U}}(x,0) = \begin{cases} \mathbf{U}_i^n & \text{if } x < 0 \\ \mathbf{U}_{i+1}^n & \text{if } x > 0 \end{cases} \end{array}\right\}, \tag{27}$$

where $\widetilde{\mathbf{J}}(\mathbf{U}_i, \mathbf{U}_{i+1})$ is a constant matrix to be determined by imposing suitable conditions.

The first derives from imposing the fulfillment of the linearized consistency condition: integrating the previous PDE system over the control volume $[-X, X] \times [0, 1]$, where X satisfies (19), one gets:

$$\int_{-X}^{+X} \widehat{\mathbf{U}}(x,1)\mathrm{d}x = X(\mathbf{U}_{i+1} + \mathbf{U}_i) - \widetilde{\mathbf{J}}(\mathbf{U}_i, \mathbf{U}_{i+1})(\mathbf{U}_{i+1} - \mathbf{U}_i).$$

Since we want to satisfy (26), the resulting constraint is

$$\text{(i) } \mathbf{F}(\mathbf{U}_{i+1}) - \mathbf{F}(\mathbf{U}_i) - \mathbf{D}_{i+1/2} = \widetilde{\mathbf{J}}(\mathbf{U}_i, \mathbf{U}_{i+1})(\mathbf{U}_{i+1} - \mathbf{U}_i). \tag{28}$$

Moreover, the following two standard requirements for the Roe method must also be fulfilled:

$$\begin{aligned} &\text{(ii) } \widetilde{\mathbf{J}}(\mathbf{U}_i, \mathbf{U}_{i+1}) && \text{has real eigenvalues and complete set of eigenvectors,} \\ &\text{(iii) } \widetilde{\mathbf{J}}(\mathbf{U}_i, \mathbf{U}_{i+1}) \to \mathbf{J}(\mathbf{U}_i) && \text{smoothly as } \mathbf{U}_{i+1} \to \mathbf{U}_i \\ & && \text{(consistency with the exact Jacobian).} \end{aligned} \tag{29}$$

It should be noticed that this formulation can be viewed as a particular specification of the general approach proposed originally by [27] for nonconservative systems. Nevertheless, since the exact Jacobian $\mathbf{J}(\mathbf{U}) = \partial\mathbf{F}/\partial\mathbf{U}$ of the original problem is not available, his indications for constructing the matrix $\widetilde{\mathbf{J}}(\mathbf{U}_i, \mathbf{U}_{i+1})$ are unfortunately useless.

We must therefore go back to the original concept of the parameter vector introduced by [21] and extend his approach to the case with nonconservative terms. The problem can be formulated as follows: given a parameter vector $\mathbf{V}$ such that both the fluxes $\mathbf{F}(\mathbf{U})$ and the conserved variables $\mathbf{U}$ can be expressed as function of $\mathbf{V}$, then we look for two matrices $\mathbf{A}, \mathbf{B}$ such that

$$\widetilde{\mathbf{J}}(\mathbf{U}_i, \mathbf{U}_{i+1}) = \mathbf{A}_{i+1/2}\mathbf{B}_{i+1/2}^{-1}, \tag{30}$$

where

$$\mathbf{A}_{i+1/2} = \mathbf{A}'_{i+1/2} + \mathbf{A}''_{i+1/2}. \tag{31}$$

In order to ensure condition (i), the following relations must be satisfied:

$$\mathbf{A}'_{i+1/2}(\mathbf{V}_{i+1} - \mathbf{V}_i) = \mathbf{F}(\mathbf{U}_{i+1}) - \mathbf{F}(\mathbf{U}_i), \tag{32a}$$
$$\mathbf{A}''_{i+1/2}(\mathbf{V}_{i+1} - \mathbf{V}_i) = -\mathbf{D}_{i+1/2}, \tag{32b}$$
$$\mathbf{B}_{i+1/2}(\mathbf{V}_{i+1} - \mathbf{V}_i) = (\mathbf{U}_{i+1} - \mathbf{U}_i). \tag{32c}$$

It is a well-known fact that in conservative systems, if every component f_i of $\mathbf{F}(\mathbf{U})$ and every component u_i of $\mathbf{U}$ can be expressed as a quadratic in the component v_i of $\mathbf{V}$, then the sought matrices are simply:

$$\mathbf{A}'_{i+1/2} = \left.\frac{\partial\mathbf{F}}{\partial\mathbf{V}}\right|_{\widetilde{\mathbf{V}}}; \quad \mathbf{B}_{i+1/2} = \left.\frac{\partial\mathbf{U}}{\partial\mathbf{W}}\right|_{\widetilde{\mathbf{V}}}, \tag{33}$$

where $\widetilde{\mathbf{V}} = 1/2(\mathbf{V}_i + \mathbf{V}_{i+1})$. Unfortunately, because of the particular structure of the fluxes and of the conserved variables and the presence of the nonconservative term in the equations, such a vector is not available for the present problem. We therefore assume as parameter vector the primitive-variable vector (Eq. (15)).

This choice allows accounting for the thrust term in a straightforward way:

$$\mathbf{A}''_{i+1/2} = \begin{bmatrix} 0 & 0 & 0 \\ 0 & 0 & 0 \\ 0 & 0 & a_{33} \end{bmatrix}, \tag{34}$$

where

$$a_{33} = g(c_k\Delta_\rho + 1)(h_k - |z_\mathrm{R} - z_\mathrm{L}|/2) \tag{35}$$

and k is defined in (18).

The determination of the other two matrices is a little more complex and must be worked out with the following ad hoc procedure:

- considering Eq. (30), the first step in order to ensure conditions (ii) and (iii) is to require that $\mathbf{A}'$ is the Jacobian matrix of $\mathbf{F}$ and $\mathbf{B}$ the Jacobian matrix of $\mathbf{U}$, written in terms of $\mathbf{W}$:

$$\mathbf{A}'_{i+1/2} = \frac{\partial\mathbf{F}}{\partial\mathbf{W}} = \begin{bmatrix} 0 & 1 & 0 \\ -d_1 u & d_1 & 0 \\ -d_2 u - u^2\left(1 - \frac{1}{2}\Delta_\rho\gamma c_\mathrm{b} g\right) + gh & d_2 + 2u & 0 \end{bmatrix}, \tag{36}$$

$$\mathbf{B}_{i+1/2} = \frac{\partial\mathbf{U}}{\partial\mathbf{W}} = \begin{bmatrix} 1 & 0 & 1 \\ -d_3 u & d_3 & c_\mathrm{b} \\ -\Delta_\rho d_1 u & \Delta_\rho d_1 + 1 & 0 \end{bmatrix}, \tag{37}$$

where $d_1 = 3c_\mathrm{b}\gamma u^2/h, d_2 = \Delta_\rho\gamma c_\mathrm{b}(gu + 4\frac{u^3}{h}), d_3 = 2c_\mathrm{b}\gamma u/h$.

- one way to ensure additionally conditions (32a) and (32c) is to find a suitable expression of the averaged state parameter vector $\widetilde{\mathbf{W}}_{i+1/2}$ such that

$$\left.\frac{\partial \mathbf{F}}{\partial \mathbf{W}}\right|_{\widetilde{\mathbf{W}}_{i+1/2}} (\mathbf{W}_{i+1} - \mathbf{W}_i) = \mathbf{F}(\mathbf{U}_{i+1}) - \mathbf{F}(\mathbf{U}_i), \tag{38a}$$

$$\left.\frac{\partial \mathbf{U}}{\partial \mathbf{W}}\right|_{\widetilde{\mathbf{W}}_{i+1/2}} (\mathbf{W}_{i+1} - \mathbf{W}_i) = (\mathbf{U}_{i+1} - \mathbf{U}_i). \tag{38b}$$

Unfortunately, it is almost impossible to obtain such a vector. Therefore, we assume a given expression of $\widetilde{\mathbf{W}}_{i+1/2}$ and we consider the quantities d_1, d_2 and d_3 in the Jacobian matrices as degrees of freedom. To avoid misunderstanding with the previous definition of these quantities, we indicate them with $\hat{d}_1, \hat{d}_2$ and $\hat{d}_3$. As with the assumption made in [1] for the fixed-bed case, we have assumed $\tilde{u} = (u_{i+1}\sqrt{h_{i+1}} + u_i\sqrt{h_i})/(\sqrt{h_{i+1}} + \sqrt{h_i})$ and the following averaged vector:

$$\widetilde{\mathbf{W}}_{i+1/2} = \begin{bmatrix} \tilde{h} \\ \tilde{q} \\ \tilde{z} \end{bmatrix}_{i+1/2} = \begin{bmatrix} \frac{1}{2}(h_{i+1} + h_i) \\ \tilde{u}_{i+1/2}\tilde{h}_{i+1/2} \\ \frac{1}{2}(z_{i+1} + z_i) \end{bmatrix}. \tag{39}$$

Matrices $\mathbf{A}'_{i+1/2}$ and $\mathbf{B}_{i+1/2}$ now become:

$$\mathbf{A}'_{i+1/2} = \left.\frac{\partial \mathbf{F}}{\partial \mathbf{W}}\right|_{\widetilde{\mathbf{W}}_{i+1/2}} = \begin{pmatrix} 0 & 1 & 0 \\ -\hat{d}_1\tilde{u} & \hat{d}_1 & 0 \\ -\hat{d}_2\tilde{u} - \tilde{u}^2(1 - \frac{1}{2}\Delta_\rho\gamma c_b g) + g\tilde{h} & \hat{d}_2 + 2\tilde{u} & 0 \end{pmatrix}, \tag{40}$$

$$\mathbf{B}_{i+1/2} = \left.\frac{\partial \mathbf{U}}{\partial \mathbf{W}}\right|_{\widetilde{\mathbf{W}}_{i+1/2}} = \begin{pmatrix} 1 & 0 & 1 \\ -\hat{d}_3\tilde{u} & \hat{d}_3 & c_b \\ -\Delta_\rho\hat{d}_1\tilde{u} & \Delta_\rho\hat{d}_1 + 1 & 0 \end{pmatrix}, \tag{41}$$

where $\hat{d}_1, \hat{d}_2$ and $\hat{d}_3$ are still unknowns. These coefficients can be determined univocally imposing (32a) and (32c); their values become:

$$\hat{d}_1 = c_b\gamma\frac{\sqrt{h_{i+1}} + \sqrt{h_i}}{\sqrt{h_{i+1}}h_i + \sqrt{h_i}h_{i+1}}(u_{i+1}^2 + u_i^2 + u_i u_{i+1}), \tag{42a}$$

$$\hat{d}_2 = \Delta_\rho\gamma c_b\left(g\tilde{u} + \frac{(u_{i+1}^2 + u_i^2)}{\sqrt{h_i h_{i+1}}}(u_i + u_{i+1})\right), \tag{42b}$$

$$\hat{d}_3 = c_b\gamma\frac{(u_{i+1} + u_i)}{\sqrt{h_i h_{i+1}}}. \tag{42c}$$

It is clear that different choices of the averaged vector $\widetilde{\mathbf{W}}_{i+1/2}$ lead to different expressions of the above quantities. Nevertheless, the above-described approach is the only one we found that also ensures fulfillment of conditions (ii) and (iii).

It is now possible to write the update algorithm as usual for Roe approaches. We define $\lambda^m_{i+1/2}$ the mth eigenvalue of the matrix (30) and $\mathbf{G}^m_{i+1/2}$ the right eigenvector associated with $\lambda^m_{i+1/2}$ (see Appendix A for their detailed expression). The solution of a linear RP can then be expressed (see e.g. [17], chapter 6) starting from the left or the right initial data adding or subtracting the values of the wave strength multiplied by the eigenvector of each wave encountered on the way from the initial value to the constant state we are interested in:

$$\widehat{\mathbf{U}}(x,t) = \mathbf{U}_{i+1} - \sum_{\lambda^m_{i+1/2} > x/t} (\mu\mathbf{G})^m_{i+1/2}, \quad m = 1,2,3,$$

$$\widehat{\mathbf{U}}(x,t) = \mathbf{U}_i + \sum_{\lambda^m_{i+1/2} < x/t} (\mu\mathbf{G})^m_{i+1/2}, \quad m = 1,2,3$$

where μ^m is the wave strength associated with the mth eigenvalue λ^m. The determination of the wave strengths can be done by projecting the total jump of the conserved variables $(\mathbf{U}_{i+1} - \mathbf{U}_i)$ onto the right eigenvectors:

$$\mathbf{U}_{i+1} - \mathbf{U}_i = \sum_{m=1,3} (\mu\mathbf{G})^m_{i+1/2}. \tag{43}$$

The detailed expression for $\mu^m_{i+1/2}$ is reported in Appendix A. Finally, the update algorithm follows from an average of the solution over the cell affected by the evolution of the side RPs located in $x_{i-1/2}, x_{i+1/2}$:

$$\mathbf{U}_i^{n+1} = \mathbf{U}_i^n - \frac{\Delta t}{\Delta x}\left(\sum_{m=1}^{3}(\lambda^+ \mu \mathbf{G})_{i-1/2}^m + \sum_{m=1}^{3}(\lambda^- \mu \mathbf{G})_{i+1/2}^m\right), \tag{44}$$

where

$$(\lambda^+)_{i-1/2}^m = (1 + \mathrm{sign}(\lambda_{i-1/2}^m))\lambda_{i-1/2}^m, \quad (\lambda^-)_{i+1/2}^m = (1 - \mathrm{sign}(\lambda_{i+1/2}^m))\lambda_{i+1/2}^m. \tag{45}$$

It should be noticed that at each time-step, because of the fact that both the nonconservative term and the Roe matrices can be expressed only in terms of primitive variables, a nonlinear system must be solved in order to go back to the primitive variables from the conserved ones. We therefore look for a more efficient algorithm which directly uses primitive variables. This approach will be presented in the following section.

3.3. The generalized Roe scheme in terms of primitive variables

Taking the primitive vector $\mathbf{W}$, defined in (15), we want to obtain an approximated solution of the homogeneous part of system (6) by solving the following locally linearized system

$$\widehat{\mathbf{B}}\frac{\partial \widetilde{\mathbf{W}}}{\partial t} + \widehat{\mathbf{A}}\frac{\partial \widetilde{\mathbf{W}}}{\partial x} = 0 \tag{46}$$

in a Roe-type framework. This means that:

- we want to solve the following side-cell, locally-linear RPs:

$$\left.\begin{array}{l} \frac{\partial \widetilde{\mathbf{W}}}{\partial t} + \mathbf{M}(\mathbf{W}_i, \mathbf{W}_{i+1})\frac{\partial \widetilde{\mathbf{W}}}{\partial x} = 0 \\ \widetilde{\mathbf{W}}(x,0) = \begin{cases} \mathbf{W}_i & \text{if } x < 0 \\ \mathbf{W}_{i+1} & \text{if } x > 0 \end{cases} \end{array}\right\}, \tag{47}$$

  where $\mathbf{M}(\mathbf{W}_i, \mathbf{W}_{i+1}) = \widehat{\mathbf{B}}_{i+1/2}^{-1}\widehat{\mathbf{A}}_{i+1/2}$;
- the solution at the new time level can be expressed directly in primitive variables by means of a cell-average procedure that leads to an expression similar to (44):

$$\mathbf{W}_i^{n+1} = \mathbf{W}_i^n - \frac{\Delta t}{\Delta x}\left(\sum_{m=1}^{3}(\hat{\lambda}^+ \hat{\mu}\mathbf{K})_{i-1/2}^m + \sum_{m=1}^{3}(\hat{\lambda}^- \hat{\mu}\mathbf{K})_{i+1/2}^m\right), \tag{48}$$

  where $\mathbf{K}_{i+1/2}^m$ is the left eigenvector associated with the mth eigenvalue $\hat{\lambda}_{i+1/2}^m$ of $\mathbf{M}(\mathbf{W}_i, \mathbf{W}_{i+1})$.

In order to obtain a good scheme, the solution of (47) must fulfill the consistency condition (26). Starting from (46) written in position $i + 1/2$, its integration of over the usual control volume $[-X, X] \times [0, 1]$ gives:

$$\int_{-X}^{+X} \widehat{\mathbf{B}}_{i+1/2}\widetilde{\mathbf{W}}\,\mathrm{d}x = X\widehat{\mathbf{B}}_{i+1/2}(\mathbf{W}_{i+1} + \mathbf{W}_i) + \widehat{\mathbf{A}}_{i+1/2}(\mathbf{W}_i - \mathbf{W}_{i+1}). \tag{49}$$

The following constraints then follow:

(a) $(\mathbf{U}_i + \mathbf{U}_{i+1}) = \widehat{\mathbf{B}}_{i+1/2}(\mathbf{W}_i + \mathbf{W}_{i+1})$,

(b) $\mathbf{F}(\mathbf{U}_i) - \mathbf{F}(\mathbf{U}_{i+1}) - \mathbf{D}_{i+1(2} = \widehat{\mathbf{A}}_{i+1/2}(\mathbf{W}_i - \mathbf{W}_{i+1})$.

We can impose two more conditions, which are standard requirements for the Roe-type methods:

(c) $\mathbf{M}(\mathbf{W}_i, \mathbf{W}_{i+1})$ has real eigenvalues and complete set of eigenvectors

(d) $\left.\begin{array}{l} \widehat{\mathbf{B}}(\mathbf{W}_i, \mathbf{W}_{i+1}) \to \frac{\partial \mathbf{U}}{\partial \mathbf{W}}(\mathbf{W}_i) \\ \widehat{\mathbf{A}}(\mathbf{W}_i, \mathbf{W}_{i+1}) \to \frac{\partial \mathbf{F}}{\partial \mathbf{W}}(\mathbf{W}_i) \end{array}\right\}$ smoothly as $\mathbf{W}_{i+1} \to \mathbf{W}_i$ (consistency with the exact Jacobians).

Finally, in analogy with (32c), and consistently with condition (d), we can require:

(e) $\widehat{\mathbf{B}}_{i+1/2}(\mathbf{W}_i - \mathbf{W}_{i+1}) = (\mathbf{U}_i - \mathbf{U}_{i+1})$. (50)

It should be noticed that the conditions imposed on $\widehat{\mathbf{A}}_{i+1/2}$ (conditions b and d) are the same as have been imposed on $\mathbf{A}_{i+1/2}$ (32a) and (32b): therefore $\widehat{\mathbf{A}}_{i+1/2} = \mathbf{A}_{i+1/2}$ and its expression is already available (Eq. (40)). As far as the matrix $\widehat{\mathbf{B}}_{i+1/2}$ is concerned, conditions (a) and (e) are sufficient to determine its nine components univocally. Unfortunately, the resulting matrix $\mathbf{M}(\mathbf{W}_i, \mathbf{W}_{i+1})$ does not satisfy condition (d) and we have used practical computations to verify that neither condition (c) is matched in several situations. The approach is therefore not usable in a straightforward manner. In order to be able to satisfy

these two last restrictions, condition (a) must be relaxed. Now the requirements for matrix $\widehat{\mathbf{B}}_{i+1/2}$ are exactly the same as those used to obtain matrix $\mathbf{B}_{i+1/2}$ (32c); therefore

$$\widehat{\mathbf{B}}_{i+1/2} = \mathbf{B}_{i+1/2} \tag{51}$$

and its expression is already available (Eq. (41)). The consistency condition is thus no longer verified and therefore the solution is not completely conservative. We end up with the following result:

$$\mathbf{M}_{i+1/2} = \mathbf{B}_{i+1/2}^{-1}\mathbf{A}_{i+1/2}. \tag{52}$$

If we compare this matrix with (30), we can deduce that both matrices present the same set of eigenvalues. Let us consider the following determinant:

$$d = \det(\mathbf{B}^{-1}\mathbf{A}\mathbf{B}^{-1} - \lambda\mathbf{I}\mathbf{B}^{-1})_{i+1/2}. \tag{53}$$

It can be written in the following two equivalent forms:

$$d = \det(\mathbf{B}^{-1})_{i+1/2}\det(\mathbf{A}\mathbf{B}^{-1} - \lambda\mathbf{I})_{i+1/2}, \tag{54}$$

$$d = \det(\mathbf{B}^{-1}\mathbf{A} - \lambda\mathbf{I})_{i+1/2}\det(\mathbf{B}_{i+1/2}^{-1}), \tag{55}$$

from which follows:

$$\det(\mathbf{B}^{-1}\mathbf{A} - \lambda\mathbf{I})_{i+1/2} = \det(\mathbf{A}\mathbf{B}^{-1} - \lambda\mathbf{I})_{i+1/2} \tag{56}$$

and then

$$\hat{\lambda}_{i+1/2}^{m} = \lambda_{i+1/2}^{m}.$$

Considering the matrix $\mathbf{M}_{i+1/2}$, the definition of its right eigenvector $\mathbf{K}_{i+1/2}^{m}$ associated with $\lambda_{i+1/2}^{m}$, is

$$(\mathbf{M}\mathbf{K}^{m})_{i+1/2} = (\lambda\mathbf{K})_{i+1/2}^{m}. \tag{57}$$

Since the eigenvector $\mathbf{G}_{i+1/2}^{m}$ of $\widetilde{\mathbf{J}}(\mathbf{U}_i, \mathbf{U}_{i+1})$ can be written as follows:

$$(\mathbf{A}\mathbf{B}^{-1})_{i+1/2}\mathbf{G}_{i+1/2}^{m} = (\lambda\mathbf{G})_{i+1/2}^{m}, \tag{58}$$

multiplying the equation on the left by $\mathbf{B}_{i+1/2}^{-1}$ one gets:

$$(\mathbf{B}^{-1}\mathbf{A})_{i+1/2}(\mathbf{B}^{-1}\mathbf{G}^{m})_{i+1/2} = \lambda_{i+1/2}^{m}(\mathbf{B}^{-1}\mathbf{G}^{m})_{i+1/2}, \tag{59}$$

using (52), this becomes:

$$\mathbf{M}_{i+1/2}(\mathbf{B}^{-1}\mathbf{G}^{m})_{i+1/2} = \lambda^{m}(\mathbf{B}^{-1}\mathbf{G}^{m})_{i+1/2}.$$

Comparing the last expression with Eq. (57), the following equality can be obtained:

$$\mathbf{G}_{i+1/2}^{m} = \mathbf{B}_{i+1/2}\mathbf{K}_{i+1/2}^{m}, \tag{60}$$

which relates the eigenvalues of matrix $\widetilde{\mathbf{J}}(\mathbf{U}_i, \mathbf{U}_{i+1})$ with those of matrix $\mathbf{M}_{i+1/2}$. It follows that the wave strengths associated with the approximated solution of RP (47) are the same as those associated with the solution of (27). In fact, by using (60) and (50), equation (43) may be rewritten as

$$\mathbf{B}_{i+1/2}(\mathbf{W}_{i+1} - \mathbf{W}_i) = \sum_{m=1,3}\mathbf{B}_{i+1/2}(\mu\mathbf{K})_{i+1/2}^{m}, \tag{61}$$

which reduces to

$$\mathbf{W}_{i+1} - \mathbf{W}_i = \sum_{m=1,3}(\mu\mathbf{K})_{i+1/2}^{m}, \tag{62}$$

which is exactly the equation that defines the wave strength for RP (47).

Finally, the resulting update algorithm (48) becomes:

$$\mathbf{W}_i^{n+1} = \mathbf{W}_i^{n} - \frac{\Delta t}{\Delta x}\left(\sum_{m=1}^{3}(\lambda^{+}\mu\mathbf{K})_{i-1/2}^{m} + \sum_{m=1}^{3}(\lambda^{-}\mu\mathbf{K})_{i+1/2}^{m}\right), \tag{63}$$

where $(\lambda^{+})_{i-1/2}^{m}$ and $(\lambda^{-})_{i+1/2}^{m}$ are defined in (45). Moreover, by using the same quantities, it is also possible to rewrite the algorithm in terms of conserved variables (44):

$$\mathbf{U}_i^{n+1} = \mathbf{U}_i^{n} - \frac{\Delta t}{\Delta x}\left(\mathbf{B}_{i-1/2}\sum_{m=1}^{3}(\lambda^{+}\mu\mathbf{K})_{i-1/2}^{m} + \mathbf{B}_{i+1/2}\sum_{m=1}^{3}(\lambda^{-}\mu\mathbf{K})_{i+1/2}^{m}\right). \tag{64}$$

In other words, by using matrices $\mathbf{A}_{i+1/2}$ and $\mathbf{B}_{i+1/2}$ as defined in the previous section, eigenstructure of $\mathbf{B}^{-1}_{i+1/2}\mathbf{A}_{i+1/2}$ and wave strengths μ^m, it is possible to obtain a Roe solver both in terms of conserved variables and in terms of primitive variables. The latter is computationally faster than the former since it does not need a backward passage from conserved to primitive variables, but is not completely conservative, as will be shown in the test Section 4.

3.4. Treatment of the friction-source term and stability condition

To express the source term we used the approach of [4,18] consisting in projecting the source term onto the eigenvectors of each side RP. In this way, a formulation with the same structure of Eq. (63) and (64) is obtained.

For the formulation in terms of conserved variables, we assume:

$$\mathbf{R}_{i+1/2}\Delta x_{i+1/2} = \mathbf{B}_{i+1/2}\sum_{m=1}^{3}(\omega\mathbf{K})^m_{i+1/2} \tag{65}$$

with

$$\mathbf{R}_{i+1/2} = (0,0,-\tilde{\tau}_{i+1/2}/\rho_w)^T, \tag{66}$$

where $\tilde{\tau}_{i+1/2}$ is a suitable explicit expression of the average bottom stress and $\Delta x_{i+1/2} = 0.5(\Delta x_{i+1} + \Delta x_i)$. Since $\mathbf{B}_{i-1/2}$ and $\mathbf{K}^m_{i+1/2}$ are already defined, the only unknowns are $\omega^m_{i+1/2}$ which can be obtained by solving the previous linear system (65). The detailed expression of $\omega^m_{i+1/2}$ is provided in Appendix A.

The complete update algorithm thus becomes:

$$\mathbf{U}_i^{n+1} = \mathbf{U}_i^n - \frac{\Delta t}{\Delta x}\left(\mathbf{B}_{i-1/2}\sum_{m=1}^{3}((\lambda^+\mu-\omega^+)\mathbf{K})^m_{i-1/2} + \mathbf{B}_{i+1/2}\sum_{m=1}^{3}((\lambda^-\mu-\omega^-)\mathbf{K})^m_{i+1/2}\right), \tag{67}$$

where

$$(\omega^+)^m_{i-1/2} = (1+\mathrm{sign}(\lambda^m_{i-1/2}))\omega^m_{i-1/2}, \quad (\omega^-)^m_{i+1/2} = (1-\mathrm{sign}(\lambda^m_{i+1/2}))\omega^m_{i+1/2}.$$

The CFL stability condition is

$$C_R = \nu\frac{\Delta t}{\Delta x} \leqslant 1, \tag{68}$$

where

$$\nu = \max_i\{\max_m\{|\lambda^{\pm}|^m_{i+1/2}\}\} \quad m = 1,2,3; \quad i = 1,\ldots,N-1 \tag{69}$$

and N is the total number of cells of the domain.

Similarly, for the formulation in terms of primitive variables, the actual friction-source term is $(\mathbf{B}^{-1}\mathbf{R})_{i+1/2}$. Its projection over the eigenvalues gives:

$$(\mathbf{B}^{-1}\mathbf{R})_{i+1/2}\Delta x_{i+1/2} = \sum_{m=1}^{3}(\hat{\omega}\mathbf{K})^m_{i+1/2}. \tag{70}$$

Nevertheless, this expression is equal to (65) and therefore:

$$\hat{\omega}^m_{i+1/2} = \omega^m_{i+1/2}.$$

The complete update algorithm then becomes:

$$\mathbf{W}_i^{n+1} = \mathbf{W}_i^n - \frac{\Delta t}{\Delta x}\left(\sum_{m=1}^{3}((\lambda^+\mu-\omega^+)\mathbf{K})^m_{i-1/2} + \sum_{m=1}^{3}((\lambda^-\mu-\omega^-)\mathbf{K})^m_{i+1/2}\right), \tag{71}$$

whose stability condition is equal to the previous scheme.

4. Numerical tests

In this section, we present a series of test cases that allow assessment of the capabilities and limits of the numerical schemes developed in the previous sections. Numerical results have been compared with exact solutions, when available, and with the results of another numerical scheme called AWB-3SRS, previously developed by two of the authors.

4.1. Brief description of the AWB-3SRS numerical scheme

For sake of completeness we here give a brief description of the AWB-3SRS scheme. Details can be found in [22].

The AWB approach provides a Godunov-type numerical scheme for the model used in this work. It belongs to the family of well-balanced schemes since it includes the nonconservative term in the solution of the Riemann problem and in the update algorithm. Two types of Riemann solvers can be used in this approach to evaluate the intercell fluxes: the Three-Shocks Riemann Solver, which leads to the AWB-3SRS formulation, and the Three-Rarefaction Riemann Solver, which leads to the AWB-3RRS one. Since the former is a little more accurate than the latter, in this work we have used the results obtained from the former only.

The 3SRS solver shares the underlying philosophy of the well-known HLL type [12] and can be considered its natural extension: the HLL method assumes that the Riemann problem, despite its actual wave-composition, is constituted by a constant central state connected to the left and to the right states by shock waves. In the 3SRS it is assumed that the RP solution is constituted by two constant inner-states and three shock-waves. The unknowns of the solution are: three shock speeds, three conserved variables (the vector $\mathbf{U}$) and three fluxes (the vector $\mathbf{F}$) for each constant state for a total of fifteen unknowns. Available relations are the generalized Rankine–Hugoniot relations (Eq. (13)) valid across each shock (for a total of nine scalar relations) and six equations linking fluxes to conserved variables in the two constant states. The solution of the resulting highly nonlinear system is overwhelmingly difficult. A way to approximate the problem is to assume an explicit estimate of the shock speeds (as in the HLL approach) as well as of the thrust terms: the number of unknowns reduces to twelve (six conserved variables and six fluxes) and the nine generalized Rankine–Hugoniot relations become linear. To end the problem, three other equations must be chosen in the set $\mathbf{F} = f(\mathbf{U})$ in both the inner-states. For the specific problem, only two linear relations can be obtained while the last is nonlinear. The authors provide a specific two-step algorithm to solve the resulting mildly nonlinear system.

4.2. Riemann problems

The first two tests are Riemann problems designed to stress the capability of the methods to capture discontinuities even when the bed-pressure term is significant. The numerical results are compared with the exact solutions and also with the results of the AWB-3SRS scheme. In these tests the bottom shear stress has been neglected in the momentum equation. The relevant exact solution has been worked out by a process of subsequent wave-field construction, starting from either initial state (left or right), and concluding with the definition of the other. In so doing an inverse problem is solved in the way outlined by [11]. The values of the initial conditions are taken from [22] and are shown in Table 1. To compete the dataset we used $\gamma = 0.01\ \mathrm{s^2/m}$, $c_b = 0.65$ and $\Delta_\rho = 1.65$. Simulations have been performed using $\Delta x = 0.1$ m and a Courant number equal to 0.95.

The self-similar solution of Test A is composed of two external rarefaction waves and a central shock. In Fig. 3 both the exact and the numerical solution obtained with the primitive-variable approach are plotted: the structure of the solution is well described and the shock is well captured, both in terms of strength and position. Both the results obtained with the conserved-variable approach and with the AWB-3SRS are very close and do not show evident differences as compared to the results of the primitive-variable approach; these results, therefore, are not shown.

In Test B the self-similar solution is composed from left to right of two rarefactions and one shock. In this case also, the exact solution is well described with all the three approaches. In Fig. 4 only the results of the primitive-variable method are shown.

In order to point out the varying accuracy of the schemes, the absolute l_2 errors have been considered. From Table 2 it is clear that in both cases the AWB-3SRS scheme achieves the best results while the conserved-variable approach is better than the primitive-variable approach. The reason for this outcome can be found in the different basic approximations of the three schemes. The Roe-type approaches use an explicit (in time) expression of $\mathbf{D}_{i+1/2}$ (see Eq. (26)) and an exact solution of a linearized RP while the AWB-3SRS is an iterative two-step approach in which each side RP is solved twice in an approximated manner, in any case maintaining the nonlinear character of the problem.

Another difference between the conserved-variable approach and the primitive-variable approach is that in the latter method conservation is not fully satisfied. In order to quantify this effect, we considered the following global balance errors:

$$\mathrm{Err} = \frac{\sum_{n=1}^{N} \Delta t^n (\mathbf{F}_{\mathrm{in}}^n - \mathbf{F}_{\mathrm{out}}^n) + \Delta x \left(\sum_{i=1}^{K} \mathbf{U}_i^0 - \sum_{k} \mathbf{U}_i^N\right)}{\sum_{n=1}^{N} \Delta t^n (\mathbf{F}_{\mathrm{in}}^n - \mathbf{F}_{\mathrm{out}}^n) + \Delta x \sum_{i=1}^{K} \mathbf{U}_i^0} 100,$$

where $\mathbf{F}_{\mathrm{in}}^n$, $\mathbf{F}_{\mathrm{out}}^n$ are the flux matrices evaluated at the boundary of the computational domain at a generic step n, N is the number of time steps, K is the total number of cells in the computational domain, Δx is the cell length and Δt^n is the time step. The previous expression is meaningful only for the first two equations of (6) because the last equation of the system is intrinsi-

Table 1
Initial values for the RP test cases

Test A			Test B		
(m)	(m/s)	(m)	(m)	(m/s)	(m)
$h_L = 2.00$	$u_L = 1.00$	$z_L = 3.00$	$h_L = 6.00$	$u_L = 0.01$	$z_L = 1.00$
$h_R = 4.00$	$u_R = 4.38$	$z_R = 2.15$	$h_R = 0.38$	$u_R = 5.01$	$z_R = 3.75$

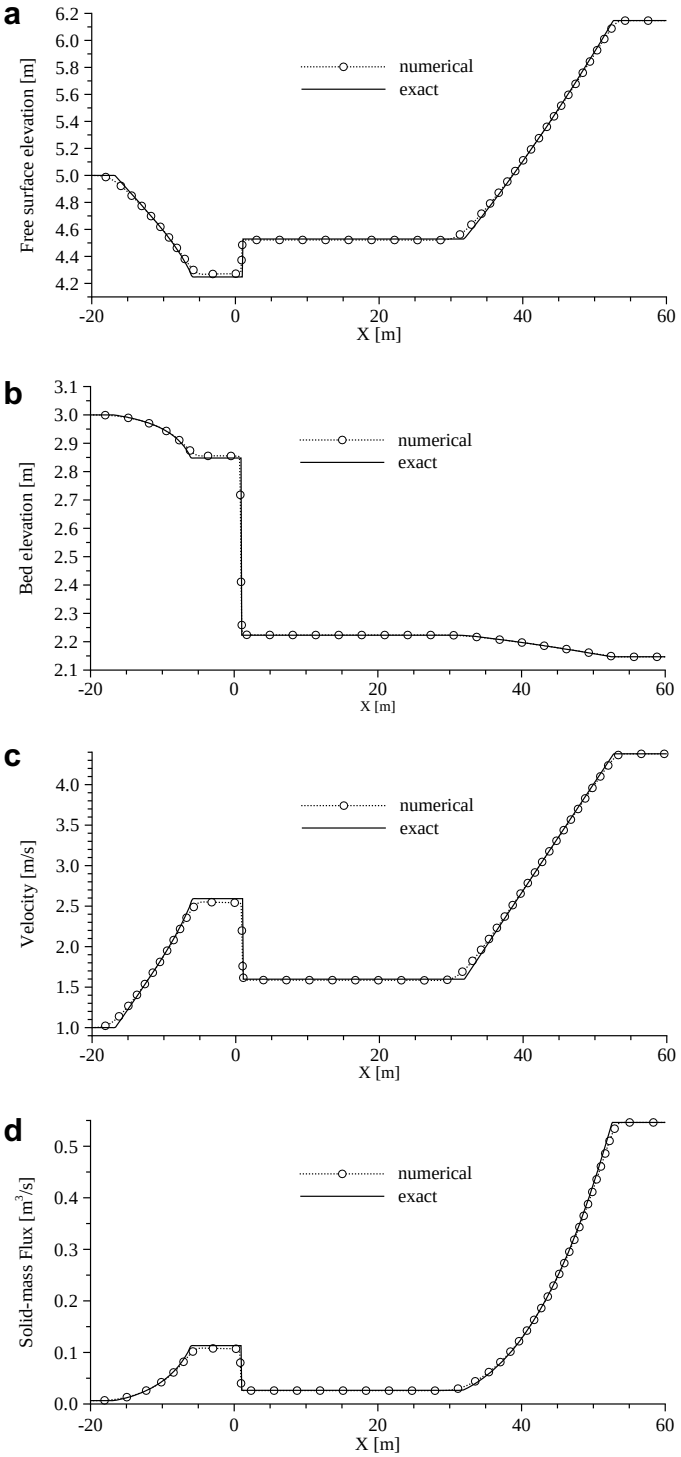

Fig. 3. Test A: comparison between exact and numerical solutions obtained with the Roe-type scheme in terms of primitive variables at $t = 5$ s.

cally nonconservative. We therefore indicate with Err_{tm} the error relevant to the first equation (expressing the total mass (tm) conservation) and with Err_{sm} the error relevant to the second equation (expressing the solid mass (sm) conservation). As can be noticed in Table 3 the order of magnitude of Err_{sm} for the primitive approach is significantly larger than the other values in both tests. Therefore, this method is not completely conservative as far as the solid mass is concerned. For short-term simulations, this error could be acceptable but the impact on long-term simulation may not be negligible.

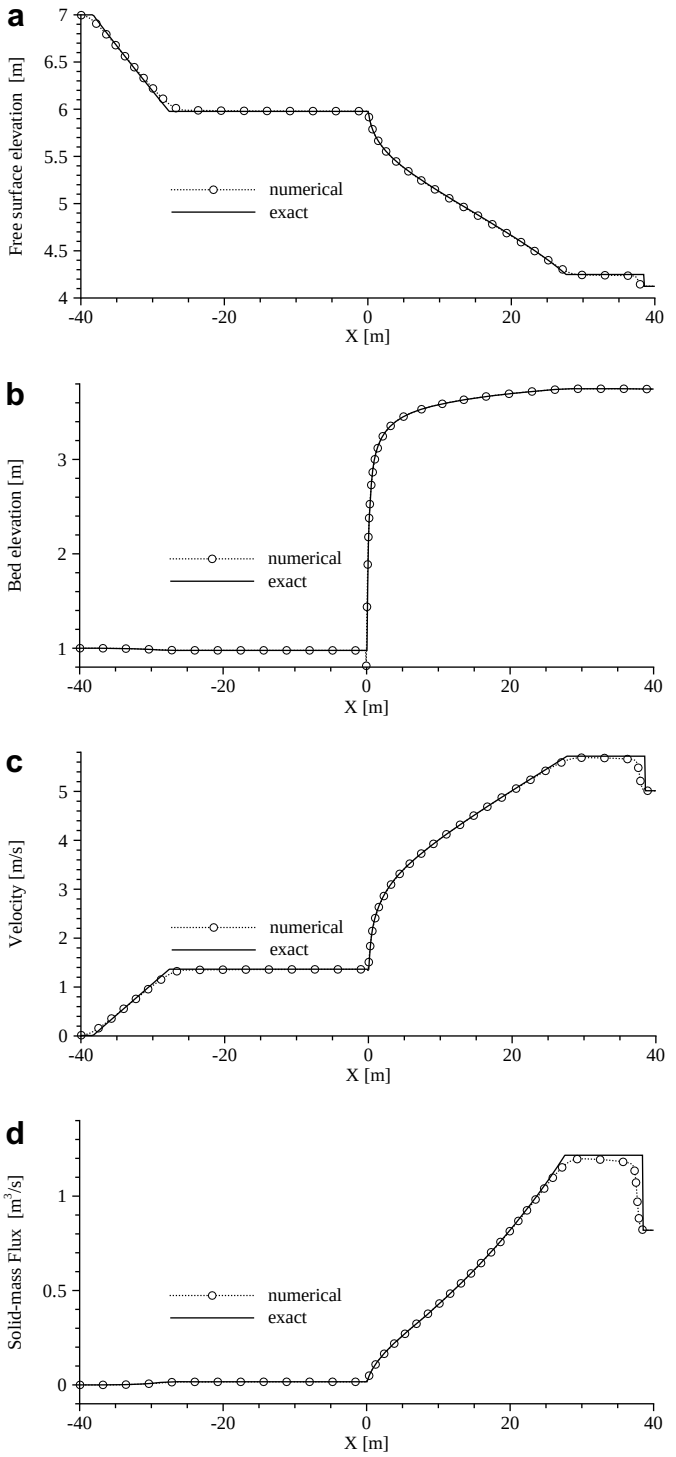

Fig. 4. Test B: comparison between exact and numerical solutions obtained with the Roe-type scheme in terms of primitive variables at $t = 5$ s.

The last aspect that characterizes the behaviour of our schemes is the computational burden. Since the nonconservative term can be expressed only in terms of the primitive variables, the conserved-variable approach needs, at each time step, a backward passage from the conserved vector to the primitive vector by solving a nonlinear system. The primitive-variable scheme is therefore much more efficient because it does not need this backward step. Furthermore, due to its double-step structure, AWB-3SRS is much heavier than the other schemes. Summarizing, the computational cost necessary for passage to a more accurate scheme is not negligible.

Table 2
Primitive-variable absolute errors (in l_2 norm) concerning Tests A and B

	Test A			Test B		
	Err_h	Err_u	Err_z	Err_h	Err_u	Err_z
Roe primitive	0.834	1.276	0.466	0.796	1.971	0.552
Roe conserved	0.744	1.188	0.394	0.790	1.640	0.578
AWB+3SRS	0.607	1.021	0.287	0.676	1.690	0.375

Table 3
Global balance relative errors at a generic timestep of the simulation concerning Tests A and B

	Test A		Test B	
	Err_{tm}	Err_{sm}	Err_{tm}	Err_{sm}
Roe primitive	0.205×10^{-11}	0.957×10^{-2}	-0.474×10^{-12}	0.477×10^{-2}
Roe conserved	0.143×10^{-11}	0.732×10^{-11}	-0.571×10^{-12}	0.282×10^{-8}

4.3. Erosional dam-break test

The dam-break flow over a mobile bed is a challenging test because of its intrinsic unsteadiness, the complexity of the interaction among water, sediments and bed surface, its relevance in practical and engineering cases and finally the possibility it offers of study in a laboratory flume [23,24]. Initial conditions for this particular Riemann problem require steady water on either side of the flow field and no water on the other side. A vertical gate allows the imposition of this condition. When the gate is removed suddenly, the subsequent flow is well described by one-dimensional shallow water, mobile-bed models [11].

This phenomenon is a benchmark case both in terms of mathematical modelling and numerical schemes. In this paper we do not aim to make a comparison between experimental and numerical results in order to stress the capability of the mathematical model, but we simply use this test case in order to highlight the limits of the primitive-variable approach as compared to the conserved approach.

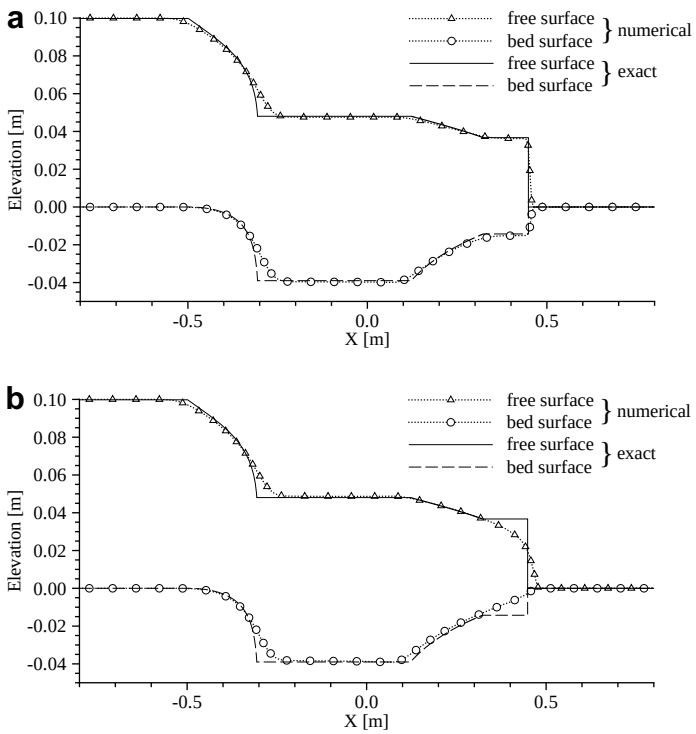

Fig. 5. Dam-break problem. Comparison between exact and numerical solutions obtained, at t=5 s, with: (a) the Roe-type scheme in terms of conserved variables; (b) Roe-type scheme in terms of primitive variables.

Table 4
Values of physical variables and parameters employed in the trench-evolution test

		Subcritical condition	Supercritical condition
Fr (Froude number)	(−)	0.85	1.2
Bed slope	(−)	8.83×10^{-3}	1.57×10^{-2}
Trench length	(m)	2	2
Trench depth	(m)	0.6	0.9
Banks slope	(−)	5	5
χ	($m^{1/2}/s$)	28.32	29.88
γ	(−)	1×10^{-4}	5×10^{-4}
h_0	(m)	2.	2.
U_0	(m/s)	3.76	5.31

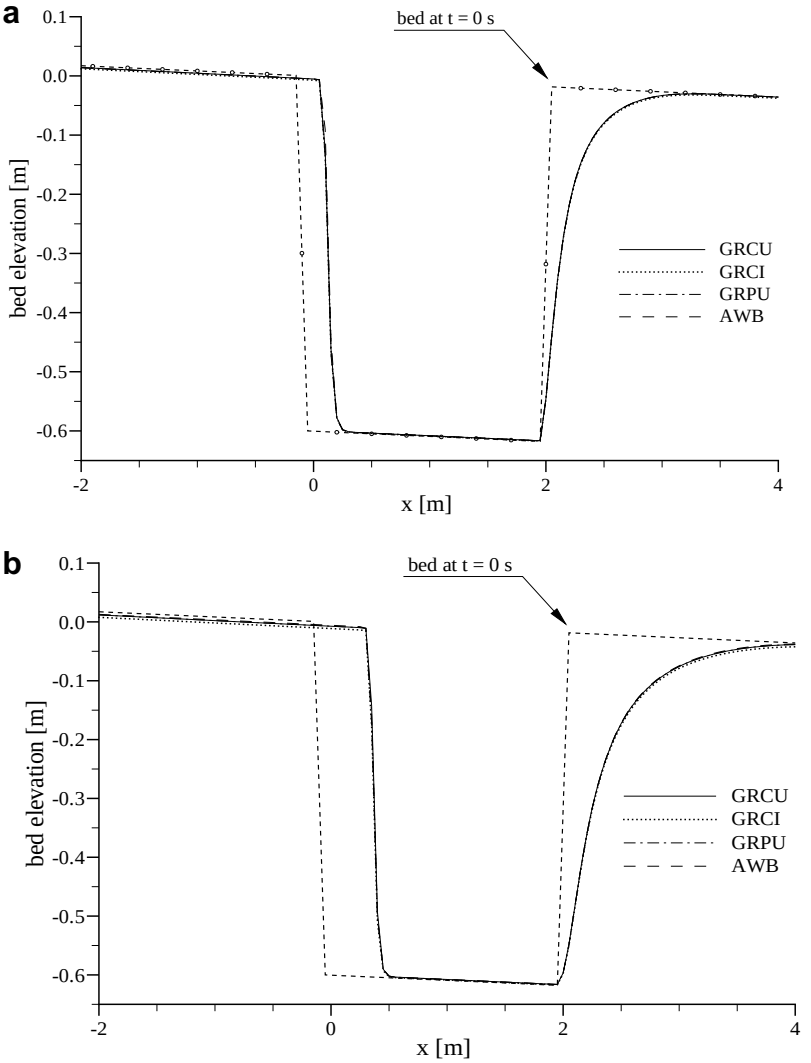

Fig. 6. Evolution of a trench in subcritical conditions: numerical solution obtained at (a) $t = 30$ s and (b) $t = 60$ s.

In the previous section we saw that the differences between the two Roe-type schemes were not remarkably large. Nevertheless, this is not true in all conditions. In this section, we present the solution of the laboratory dam-break case described in [6]. Specifically this test is characterized by an initial depth $h_0 = 0.1$m, $\rho_s = 1048$ kg/m^3, $c_b = 0.5$ and $\beta = 0.125$. In Fig. 5 the resulst of the two Roe-type schemes, obtained at t=5 s with CFL=0.9, are plotted against the exact solution. It is clear that in this realistic condition, the conserved-variable approach is much more accurate near the front respect to the primitive-variable approach presenting a smeared profile and a wrong shock speed.

4.4. Evolution of a trench

The tests presented in this section regard the evolution of a trench schematized as a big cavity in the bed with assigned geometry. The goal of these tests is to evaluate the performances of the proposed schemes in realistic physical conditions where the friction-source term plays an important role. In particular, we want to show the differences between the solutions obtained by using centered and upwind treatments of the friction-source term. The exact solution of these tests are not available but, since they have been already dealt in [22], the AWB solutions can be used for the comparison with our generalized Roe schemes. For sake of clarity and completeness, we herein provide a description of the tests.

The trench has an initial trapezoidal shape and a straight bed line with the same slope as the external domain. The initial banks of the trench are very steep. Up- and downstream reaches of the trench present uniform conditions and are long enough to rule out the influence of boundary conditions. The flow is strongly unsteady after the start, and then it develops toward asymptotic uniform conditions. As the flow evolves, the bottom friction term plays an ever more important role. Its local value has been computed by means of the Chézy formulation,

$$\frac{\tau}{\rho_w} = \frac{g}{\chi^2} u^2, \tag{72}$$

being $\chi[m^{1/2}/s]$ the Chézy friction factor. Initial conditions consist, on either side of the trench, of the uniform flow depth h_0 and velocity U_0 given in Table 4. The bed slope is consistent with Eq. (72), while the other parameters in the Table 4 allow calculation of the sediment transport and the sediment concentration in the same uniform reaches. A volumetric discharge equal to $U_0 h_0$ is initially imposed in the trench, with a straight free-surface line tilted with slope i_f and aligned with the free-surface outside the trench; the flow depth is therefore initially greater in the trench, and the velocity, as a consequence, smaller.

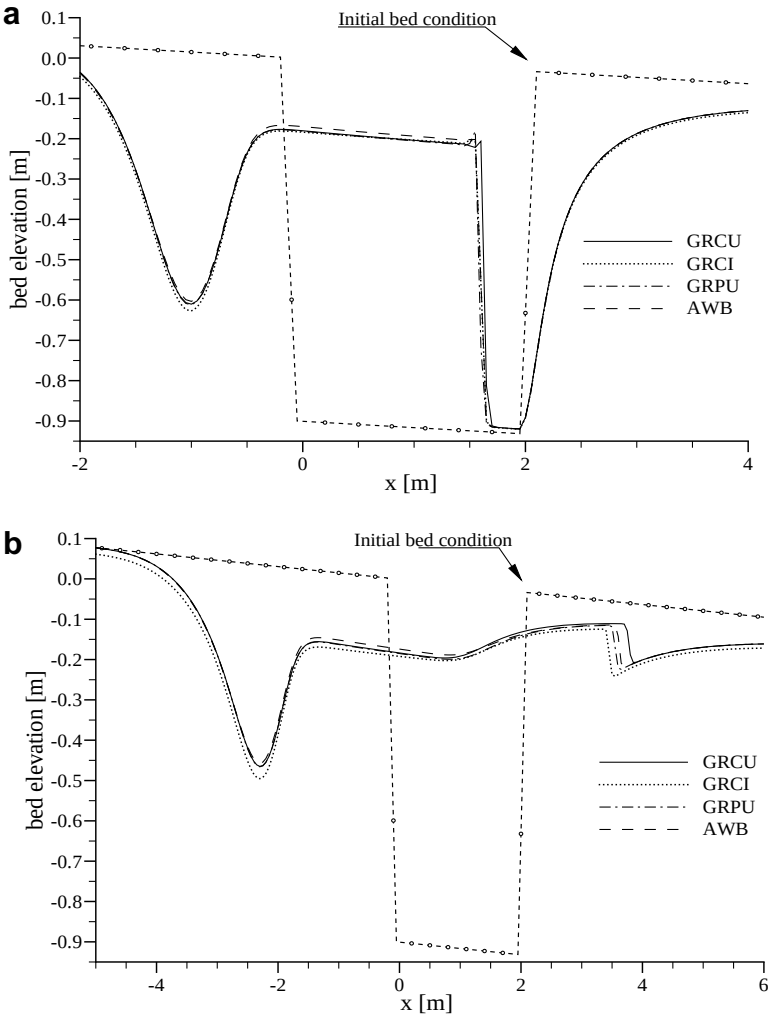

Fig. 7. Evolution of a trench in supercritical conditions: numerical solution obtained, at (a) $t = 10$ s and (b) $t = 20$ s.

Waves soon arise from the two banks of the trench and soon interact with each other, giving rise to compound structures: some of them run the flow domain toward the upstream end, the remainder toward the downstream end. The shape and speed of these compound waves evolve in a way which depends both on the trench geometry and the features of the basic uniform flows, in particular the Froude number.

The following numerical simulations have been performed using cell width $\Delta x = 0.05$ m and a CFL coefficient equal to 0.95. The methods used in the comparison are: the generalized Roe method written in terms of the conserved variables and with the upwind expression of the friction term (GRCU, Eq. (67)); the generalized Roe method written in terms of primitive variables and with the upwind expression of the friction term (GRPU, Eq. (71)); the AWB method [22]. Since in the AWB method the friction term is considered in a centered, implicit way (see [22] for details), we have also implemented a version of the generalized Roe method in terms of conserved variables in which the friction term is evaluated in the same implicit way as the AWB method (GRCI).

Fig. 6 presents the numerical evolution of the bed profile at two different times, obtained with the different methods. The behaviour of the schemes is remarkably similar and only minor differences are apparent: for instance GRCI tends to underestimate the solution on both sides. Differences arise in the supercritical case: at $t = 10$ s (Fig. 7a) all the generalized Roe schemes show a small overshoot near the steep front of the downstream compound wave (not present with the AWB scheme) and the position is also affected by the choice of scheme. The generalized Roe schemes in the central part of the solution as well as in the upstream compound wave underestimate the solution as compared to the AWB scheme. At $t = 20$ s the differences are more evident throughout the solution and, in particular, the steep front of the downstream wave shows significant differences in both position and strength. Moreover, the GRCI gives a systematic underestimation of the solution as compared to the other schemes.

Summarizing, in these last tests the schematization of the source friction term plays a significant role for the generalized Roe schemes in terms of conserved variables only in certain situations, while, somewhat surprisingly, the GRPU scheme gives solutions that are closer to the AWB-3SRS solutions than the GRCU and the GRCI schemes.

5. Conclusions

In this paper, we have dealt with the problem of constructing generalized Roe-type schemes for the problem of flows over a mobile bed with high sediment transport. The relevant PDEs system presents a nonconservative term and a highly nonlinear relation between conserved and primitive variables. From the analysis of the properties of the weak solutions of the system, we have derived the necessary conditions for obtaining generalized Roe-type solvers. The friction-source term has been included by using an upwind approach.

Two different schemes have been built using the same set of matrices, one in terms of conserved variables and one in terms of primitive variables. The capabilities and the limits of the two schemes have been highlighted comparing their results with exact solutions and with the numerical result of the AWB-3SRS. The main advantages of the proposed Roe schemes as compared to the AWB-3SRS are simplicity and efficiency. In particular, the efficiency of primitive-variable scheme is due to the absence of the implicit nonlinear passage from conserved variables to primitive variables that affect the other two methods, while the conserved-variable Roe version is more efficient than AWB because it is a single-step algorithm and not a two-step one like AWB. On the other hand, the main drawbacks of the new methods are their lower accuracy as compared to AWB-3SRS and in particular the lack of complete conservation in the primitive-variable version.

Since both accuracy and efficiency are important in practical applications, the main challenge of our future work is to develop a solver that is able to combine the efficiency of the primitive Roe-type with the accuracy of the AWB and to extend the method to a two-dimensional approach with high-order accuracy.

Acknowledgment

The present work has been partially supported by the E.C. IRASMOS Project – VI Framework Programme No. 018412.

Appendix A. Eigenstructure of $\mathbf{A}_{i+1/2}\mathbf{B}^{-1}_{i+1/2}$

The eigenvalues of matrix (30) are calculated from the third-order polynomial:

$$P(\lambda) = b_3\lambda^3 + b_2\lambda^2 + b_1\lambda + b_0 = 0, \tag{73}$$

where

$$\begin{aligned}
b_3 &= -2(c_b(1+\Delta_\rho \hat{d}_1) + \tilde{u}\hat{d}_3),\\
b_2 &= c_1\hat{d}_3 + 2(\tilde{u}\hat{d}_1(\Delta_\rho c_b + 1) + \hat{d}_2 c_b) + 4c_b\tilde{u},\\
b_1 &= -c_1 d_1 + 2(-u(uc_b - d_3 a_{33} + d_2 c_b) + ghc_b) + g\Delta_\rho \beta u^2 c_b^2,\\
b_0 &= -2\tilde{u}d_1 a_{33}
\end{aligned}$$

and $c_1 = \tilde{u}^2(g\Delta_\rho\beta c_b + 2) + 2g\tilde{h} - 2a_{33}$ while the parameters $\hat{d}_1, \hat{d}_2, \hat{d}_3$ are defined in (42) and a_{33} in (35).

The right eigenvector of (30) associated with each λ^m eigenvalue, with $m = 1, 2, 3$, is given by (60) where:

$$\mathbf{K}^m_{i+1/2} = \begin{pmatrix} \lambda^m(\hat{d}_1 - c_b - \hat{d}_3\lambda^m) \\ \lambda^m(\hat{d}_1\tilde{u} - \lambda^m(c_b + \hat{d}_3\tilde{u})) \\ (\tilde{u} - \lambda^m)(\hat{d}_1 - \hat{d}_3\lambda^m) \end{pmatrix}, \tag{74}$$

while the wave strength associated with each λ^m is

$$\mu^m = \frac{\mathbf{P}^T \cdot (\mathbf{W}_{i+1} - \mathbf{W}_i)}{p_4}, \tag{75}$$

where assuming $a \neq b \neq m$,

$$\mathbf{P} = \begin{bmatrix} c_b\hat{d}_1((\lambda^a\lambda^b - \tilde{u}(\lambda^a + \lambda^b))(\tilde{u}\hat{d}_3 + c_b(\Delta_\rho\hat{d}_1 + 1)) \\ +\tilde{u}^2\hat{d}_1(\Delta_\rho c_b + 1)) \\ \\ \tilde{u}\hat{d}_1(\lambda^a + \lambda^b)(\tilde{u}\hat{d}_3 + c_b(\Delta_\rho\hat{d}_1 + 1)) - \lambda^a\lambda^b(c_b^2(\Delta_\rho\hat{d}_1 + 1) \\ +\tilde{u}\hat{d}_3(c_b + \tilde{u}\hat{d}_3 + c_b(\Delta_\rho\hat{d}_1 + 1))) - \tilde{u}^2\hat{d}_1^2(\Delta_\rho c_b + 1) \\ \\ c_b\tilde{u}\hat{d}_1(c_b - \hat{d}_1 + \tilde{u}\hat{d}_3) \end{bmatrix},$$

$$p_4 = -c_b\tilde{u}\hat{d}_1(\lambda^a - \lambda^m)(\lambda^b - \lambda^m)(\tilde{u}\hat{d}_3 + c_b(\Delta_\rho\hat{d}_1 + 1))(c_b - \hat{d}_1 + \tilde{u}\hat{d}_3).$$

Finally, the friction strength is

$$\omega^m = \frac{-\tilde{\tau}\Delta x}{\rho_w(\lambda^a - \lambda^m)(\lambda^b - \lambda^m)(\hat{d}_3\tilde{u} + c_b(\Delta_\rho\hat{d}_1 + 1))} \tag{76}$$

In the case of wet-dry fronts, where either h_{i+1} or h_i are nil, no sediment transport is considered and the system of equations (1) reduce to the classical shallow-water equations. In this case, we use the approach proposed in [18].

References

[1] F. Alcrudo, P. García-Navarro, Flux difference splitting for 1D open channel flow equations, International Journal for Numerical Methods in Fluids 14 (1992) 1009–1018.
[2] A. Armanini, L. Fraccarollo, G. Rosatti, Two-dimensional simulation of debris flows in erodible channels, Computers and Geosciences, doi:10.1016/j.cageo.2007.11.008 (in press).
[3] P. Brufau, P. García-Navarro, P. Ghilardi, L. Natale, F. Savi, 1D mathematical modelling of debris flow, Journal of Hydraulic Research 38 (6) (2000) 435–446.
[4] J. Burguete, P. García-Navarro, Efficient construction of high-resolution TVD conservative schemes for equations with source terms: Application to shallow water flows, International Journal for Numerical Methods in Fluids 37 (2001) 209–248.
[5] Z. Cao, G. Pender, S. Wallis, P. Carling, Computational dam-break hydraulics over erodible sediment bed, Journal of Hydraulic Engineering 13 (7) (2004) 689–703.
[6] H. Capart, D.L. Young, Formation of a jump by the dam-break wave over a granular bed, Journal of Fluid Mechanics 372 (1998) 165–187.
[7] M. Castro, A.P. Milanés, C. Parés, Well-balanced numerical schemes based on a generalized hydrostatic reconstruction technique, Mathematical Models and Methods in Applied Science 17 (2007) 2055–2113.
[8] J.F. Colombeau, A.Y. LeRoux, Numerical techniques in elastoplasticity, in: Non-Linear Hyperbolic Problems, Lecture Notes in Mathematics, vol. 1270, Springer-Verlag, New York/Berlin, 1987, pp. 103–114.
[9] N. Črnjarić-Žic, S. Vucović, L. Sopta, Extension of ENO and WENO schemes to one-dimensional sediment transport equation, Computers and Fluids 33 (2004) 31–56.
[10] G. Dal Maso, P. LeFloch, F. Murat, Definition and weak stability of nonconservative products, Journal de Mathematiques Pures et Appliquees 74 (1995) 483–548.
[11] L. Fraccarollo, H. Capart, Riemann wave description of erosional dam-break flows, Journal of Fluid Mechanics 461 (2002) 183–228.
[12] A. Harten, P.D. Lax, B. Van Leer, On upstream differencing and Godunov-type schemes for hyperbolic conservation laws, SIAM Review 25 (1) (1983) 35–61.
[13] J. Hudson, P. Sweby, Formulations for numerically approximating hyperbolic systems governing sediment transport, Journal of Scientific Computing 19 (2003) 225–252.
[14] O. Hungr, A model for the runout analysis of rapid flow slides, debris flows, and avalanches, Canadian Geotechnical Journal 32 (1995) 610–623.
[15] R. Iverson, The physics of debris flows, Reviews of Geophysics 35 (1997) 245–296.
[16] Ph. Le Floch, Entropy weak solutions to nonlinear hyperbolic systems under nonconservative form, Communications in Partial Differential Equations 13 (1988) 669–727.
[17] R.J. LeVeque, Numerical Methods for Conservation Laws, Birkhäusen Verlag, 1992.
[18] J. Murillo, P. García-Navarro, J. Burguete, P. Brufau, The influence of source terms on stability, accuracy and conservation in two-dimensional shallow flow using triangular finite volumes, International Journal for Numerical Methods in Fluids 54 (2007) 543–590.
[19] C. Parés, M. Castro, On the well-balance property of Roe's method for nonconservative hyperbolic systems. Applications to shallow-water systems, ESAIM:M2AN 38 (5) (2004) 821–852.
[20] C. Parés, Numerical methods for nonconservative hyperbolic systems: A theoretical framework, SIAM Journal of Numerical Analysis 44 (1) (2006) 300–321.
[21] P. Roe, Approximate Riemann solvers, parameter vectors, and difference schemes, Journal of Computational Physics 43 (1981) 357–372.
[22] G. Rosatti, L. Fraccarollo, A well-balanced approach for flows over mobile-bed with high sediment transport, Journal of Computational Physics 220 (2006) 312–338.

[23] S. Soares-Frazão, N. le Grelle, B. Spinewine, Y. Zech, Dam-break induced morphological changes in a channel with uniform sediments: measurements by a laser-sheet imaging technique, Journal of Hydraulic Research 45 (SI) (2007) 87–95.
[24] B. Spinewine, Y. Zech, Small-scale laboratory dam-break waves on movable beds, Journal of Hydraulic Research 45 (SI) (2007) 73–86.
[25] B.M. Sumer, A. Kozakiewicz, J. Fredsøe, R. Deigaard, Velocity and concentration profiles in sheet-flow layer of movable bed, Journal of Hydraulic Engineering 122 (1996) 549–558.
[26] T. Takahashi, Mechanical characteristics of debris flow, Journal of Hydraulic Division ASCE 104 (8) (1978) 1153–1169.
[27] I. Toumi, A weak formulation of Roe's approximate Riemann solver, Journal of Computational Physics 102 (1992) 360–373.